

## PDF hosted at the Radboud Repository of the Radboud University Nijmegen

The following full text is a publisher's version.

For additional information about this publication click this link.

<http://hdl.handle.net/2066/92624>

Please be advised that this information was generated on 2017-12-06 and may be subject to change.

## Local probing of the polarization state in thin $\text{Pb}(\text{ZrTi})\text{O}_3$ films during polarization reversal

E. D. Mishina, N. E. Sherstyuk, E. Ph. Pevtsov, K. A. Vorotilov, and A. S. Sigov  
*Moscow Institute of Radioengineering, Electronics and Automation, Moscow 117454, Russia*

M. P. Moret, S. A. Rössinger, P. K. Larsen, and Th. Rasing<sup>a)</sup>  
*Research Institute for Materials, University of Nijmegen, Toernooiveld 1, NL-6525 ED Nijmegen,  
 The Netherlands*

(Received 12 May 2000; accepted for publication 9 October 2000)

The polarization state of a thin  $\text{Pb}(\text{ZrTi})\text{O}_3$  film is probed by optical second-harmonic generation (SHG) while applying an external voltage (a sine wave). A hysteresis in the SHG intensity is observed that corresponds to the dielectric hysteresis and is analyzed using a phenomenological relation between the SHG intensity and the dielectric polarization. Based on this model, the polarization state of the film during polarization reversal is mapped. © 2001 American Institute of Physics. [DOI: 10.1063/1.1329332]

Dielectric polarization hysteresis is the fundamental property that enables the operation of ferroelectric-based memories.  $\text{Pb}(\text{Zr,Ti})\text{O}_3$  (PZT) is one of the promising candidates for ferroelectric-based microelectronic devices as the required switchable polarization for device operation is relatively large. Polarization switching is determined largely by the formation of domains and depends strongly on the microstructure of the films. This dependence requires noninvasive and quick control of the structure and dielectric properties. Conventional characterization techniques such as x-ray diffraction, electron microscopy, and dielectric methods probe either the structure or the electrical properties. Existing structural techniques, however, are not able to provide dielectric information, and vice versa. To investigate the structure-properties relation of materials, it would be very advantageous to have an analysis technique for thin films that can probe both in a quick and noninvasive way. Optical second-harmonic generation (SHG) has already been used for *ex situ* study of domain structures in ferroelectric and ferromagnetic films. In materials with micron-scale domains ( $\text{LiNbO}_3$ ,  $\text{LiTaO}_3$ , and magnetic garnets), a direct SHG microscopic imaging of domain structures has been demonstrated.<sup>1,2</sup> Only a very few papers are devoted to *in situ* characterization of the rearrangement of nanoscale domains during in-plane polarization of ferroelectric films by an external voltage.<sup>3</sup> Since the very first SHG studies of ferroelectric crystals,<sup>4</sup> it was shown that the SHG response is connected with the spontaneous dielectric (DE) polarization. However, the effects of the nanodomain structure on the nonlinear-optical properties is still unclear. To use SHG as a probe for local *in situ* characterization of technologically relevant properties such as polarization switching, fatigue, and microstructure, it is necessary to find a correlation between SHG parameters, DE polarization, and the domain structure. Therefore, simultaneous DE and SHG studies are required.

In this letter, we report the results of *in situ* SHG studies on thin PZT films during polarization reversal in the normal

(to the film surface) direction. A phenomenological model describing the SHG intensity as a function of the DE polarization, itself a function of the domain distribution, is presented. Based on these studies, a nonlinear-optical technique for mapping the DE polarization in thin ferroelectric films is suggested and demonstrated.

Sol-gel thin  $\text{PbZr}_{0.53}\text{Ti}_{0.47}\text{O}_3$  films were grown on a platinumized silicon substrate and annealed at 650 °C. Ellipsometry gave a film thickness of  $200 \pm 20$  nm. X-ray diffraction studies showed the presence of a texture with grains in the tetragonal phase ( $4mm$  point symmetry) with a dominant presence of (111) planes. Transmission electron microscopy (TEM) images showed a column-like structure with an average grain size of about 200 nm. The roughness of the film, measured by atomic-force microscopy, was about 20 nm. Semitransparent nickel electrodes (3 nm thick and 0.5 mm diam) were used as top electrodes. Thicker nickel electrodes (200 nm thick and 150 nm diam) were sputtered in contact with the thin ones for bonding purposes.

SHG measurements were performed using a Ti:sapphire laser at 760 nm with a pulse width of about 100 fs, a repetition rate of 82 MHz, and an average power of 100 mW focused onto a spot of about 75  $\mu\text{m}$  diam. The reflected SHG signal at 380 nm was filtered by color filters and a monochromator and detected by a photomultiplier tube. Both the fundamental and the SHG waves were polarized in the plane of incidence (*p*-in, *p*-out polarization combination). Rotation of the sample around its normal showed a completely isotropic SHG intensity, which points to a random in-plane distribution of microcrystallites without any predominant orientation.<sup>5</sup> Scattering indicatrices were not affected by the evaporation of the thin electrodes and showed that the SHG signal is 99.5% specular (within the accuracy of an aperture that is about 2°).

The dielectric hysteresis loops were measured using a Sawyer-Tower circuit; an external low-frequency voltage from a function generator was applied to a ferroelectric capacitor at  $1/\tau_{\text{ext}} = 1$  kHz. In order to scan a dielectric hysteresis loop with the SHG probe, the photon-counting detection was gated with the gate width  $\tau_{\text{gate}} = 0.01\text{--}0.02$  ms. The gate

<sup>a)</sup>Electronic mail: mariloub@sci.kun.nl

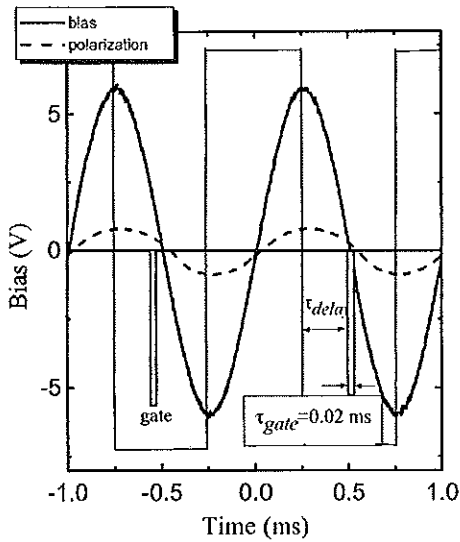


FIG. 1. Schematic of the SHG and DE hysteresis synchronization. The solid line is the sine wave of the external bias; the dashed line is the DE polarization measured with the Sawyer-Tower technique. The superimposed thin solid line is the synchronization signal from the function generator that initiates the photon-counter detection cycle. The thin rectangle is the gate of the photon counter that can be changed in width and delay with respect to triggering pulse.

was triggered by the function generator, and the gate delay could be varied within  $\tau_{ext}$  with a step  $\tau_{del}=0.02-0.05$  ms (see Fig. 1).

The SHG signal from the nickel electrode was ten times smaller than the signal from the uncovered and unbiased PZT film. Upon application of an electric field this difference became even larger up to an order of magnitude for high biases ( $\pm 6$  V). Therefore, we attributed the whole SHG intensity to the PZT film and ignored the background signal from the electrodes.

Figure 2 (left-top panel) shows the bias dependences of the SHG intensity  $I^{2\omega}(U)$ , displaying SHG hysteresis loops that correspond to the DE hysteresis loops (left-bottom panel). The right panel shows the SHG intensity as a function of DE polarization  $P$ . The  $I^{2\omega}(P)$  dependences are co-

incident for all amplitudes of external bias and do not show any hysteresis. This means that in contrast to  $I^{2\omega}(U)$ , the dependence of the SHG intensity on  $P$  is unambiguous in our films and, consequently, the SHG intensity can be used as a measure of this DE polarization. Thus, once we know the relation  $I^{2\omega}(P)$ , we can use the SHG response to locally probe the polarization state of the PZT film, with a resolution that is given by the area of the laser spot. Figure 3 shows the evolution of the polarization reversal as obtained from SHG maps of the sample for external biases  $U=6, 0, -6$ , and  $0$  V. The areas with thick electrodes are clearly seen as dark spots. The brightness of the polarized area is clearly inhomogeneous. The contrast of the pictures is well above the thickness inhomogeneity (roughness) and indicates an inhomogeneous DE polarization. Figures 3(b) and 3(d) correspond to zero external bias, giving in this way a map of the spontaneous polarization of opposite sign. These polarization maps were obtained from the experimental SHG maps using the modeling as sketched below. TEM images showed that the PZT films consisted of microcrystallites of antiparallel (“+” and “-”) lamellar twin domains. Crystallographically, they are equal to (111) and  $1\bar{1}\bar{1}$  faces for + and - domains. The thickness  $d_{\pm}$  of a  $\pm$ -type domain depends on the DE polarization. For a film divided into  $N$  twin domains along the film (grain) normal  $d_{+}=d(1-P_n)/2N$  and  $d_{-}=d(1+P_n)/2N$ , where  $P_n$  is the normalized DE polarization and  $d$  is the film thickness.<sup>6</sup> In this model, the DE polarization dependence of the SHG intensity arises due to bias-induced redistribution of + and - domains only. This contribution can be called a crystallographic contribution similarly to magnetic materials.<sup>2</sup> The direct contribution of electric-field-induced polarization is negligibly small in comparison with the crystallographic contribution in our samples.

For a random in-plane distribution of the microcrystallites the SHG field is a random function and, therefore, an averaging over the laser spot with a random distribution function is required:

$$I^{2\omega} \propto \langle E(2\omega, \Psi) \rangle^2 + \langle E^2(2\omega, \Psi) \rangle \propto \langle \chi(\Psi) \rangle^2 + \langle \chi^2(\Psi) \rangle, \quad (1)$$

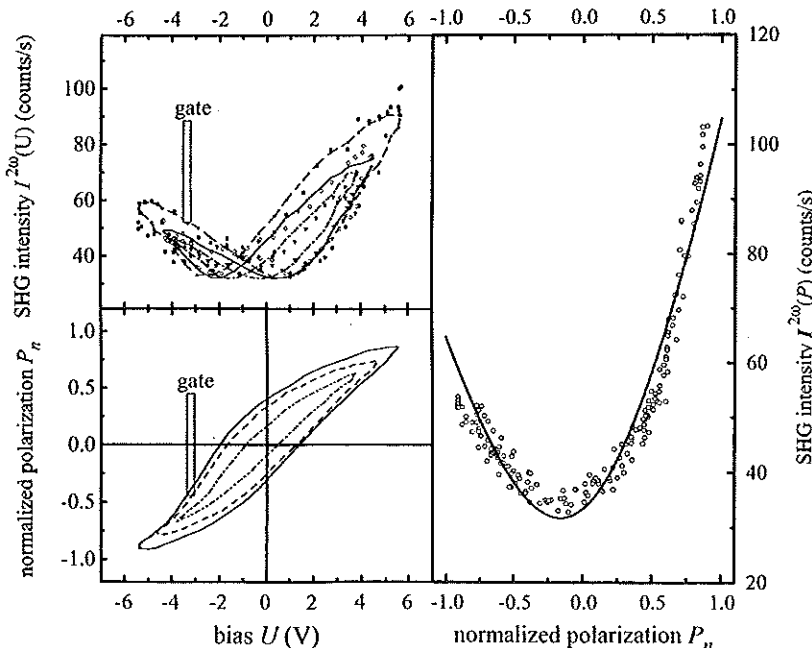


FIG. 2. Left panels: SHG hysteresis loops (top panel) measured in the same point of the sample for different DE hysteresis loops (bottom panel). The three lines, in the top and bottom panels, represent the fit to our model and correspond to each other with respect to their shape. Right panel: SHG intensity (experimental points and fit) as a function of DE polarization obtained from the appropriate hysteresis loops from the left panel. The thin rectangle is the gate of the photon counter that can be changed in width and delay with respect to triggering pulse.

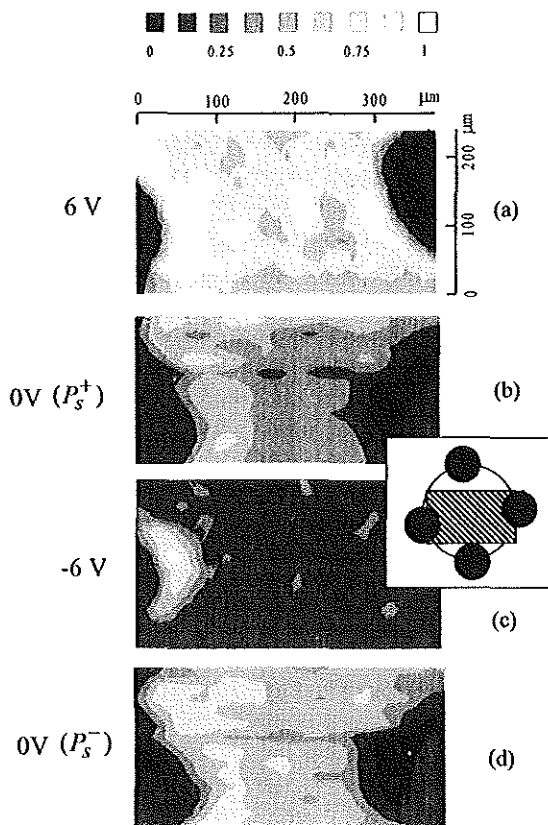


FIG. 3. SHG maps of the sample polarization measured at various points in the hysteresis loop ( $-6, 0, +6, 0$  V). The legend on the right shows the electrode schematic with respect to the mapping. The dark areas in the maps correspond to the thick nickel electrodes that give a negligible SHG signal. The contrast of the maps corresponds to the error bars in the polarization.

where  $\Psi$  is the azimuthal angle in the surface frame. The first term in Eq. (1) gives the coherent SHG signal, the second one corresponds to the incoherent contribution  $I_{\text{inc}}^{2\omega}$ . The incoherent contribution  $\langle \chi^2(\Psi) \rangle = \chi_{\text{inc}}^2$  is equal for both types of domains. For the coherent contribution averaging gives  $\Psi$ -independent effective nonlinear susceptibilities  $\langle \chi(\Psi) \rangle = \pm \chi_0$  (with + and - corresponding to + and - domains, respectively, within a single grain). The coherent contribution to the SHG intensity is a result of a summation of the SHG field over all domains and can be calculated in a similar way as in Ref. 7. This gives a parabolic dependence of the SHG intensity as a function of DE polarization with  $I^{2\omega} = 0$  at  $P_n = 0$ . In the experimental  $I^{2\omega}(P)$  dependences, the minimum is shifted by  $\Delta P_n = 0.15$  from zero. This means that there exists an initial (unswitchable) polarization  $\Delta P_n$  due to internal electric fields and strain, which is consistent with earlier studies.<sup>8</sup> Therefore, the SHG intensity in our films is described by

$$I^{2\omega} \propto \chi_{\text{inc}}^2 / \chi_0^2 + (P_n + \Delta P_n)^2. \quad (2)$$

The solid line in Fig. 2 (right panel) is a fit to Eq. (2). Figure 2 (left panel) shows the same dependence but plotted as a function of external bias for the appropriate DE hysteresis loops. Only three (the same for all dependences) fitting pa-

rameters were used: the number of twin domains through the film thickness, the ratio of  $\chi_{\text{inc}}^2 / \chi_0^2$ , and  $\Delta P_n$ . Knowing the relation between the polarization and the SHG intensity, we can use  $I^{2\omega}$  to locally measure the polarization state of the PZT film, as was done in Fig. 3. Experimentally, we found that the incoherent radiation falls within the aperture of our detection system from this, the correlation length of the nonlinear sources for our films can be estimated to be more than  $1 \mu\text{m}$ .<sup>9</sup> Such a long-scale length may arise from an in-plane distribution of internal electric fields and/or strain due to the preparation procedure.

It is important to note that internal fields are not able to change directly the SHG field as was suggested in Ref. 10. This is because for noncentrosymmetric media the higher-order components  $\chi_{ijkl} E_j(\omega) E_k(\omega) E_0 + p_{ijklm} E_j(\omega) E_k(\omega) u_{lm}$  are much smaller than the second-order crystallographic contribution (here,  $E_0$  is the low-frequency electric field,  $u_{lm}$  the strain tensor, and  $\chi_{ijkl}$  and  $p_{ijklm}$  are appropriate susceptibility tensors). However, these fields do influence, through domain formation, the total polarization and, therefore, the SHG intensity.

To conclude, we have developed a technique for *in situ* measurements of SHG during polarization reversal and have shown that the SHG intensity is a direct measure of the local DE polarization in ferroelectric-biased polycrystalline thin films. We showed that with an applied external bias a crystallographic contribution to the SHG field remains dominant. We have demonstrated the application of this technique for a spatially resolved mapping of the polarization state during polarization reversal in thin ferroelectric films. Spatial resolution of this probe can be improved down to the diffraction limit of about  $0.5 \mu\text{m}$ . Based on these studies, a qualitative, quick contactless mapping of polarization state is also possible.

The authors are indebted to P. Mulder and J. Schermer for the expertise with the electrode preparation. The authors would like to thank Dr. A. V. Petukhov for useful discussions. One of the authors (E.D.M.) thanks the Research Institute for Materials of the University of Nijmegen for their hospitality. This work is supported by NWO and RFBR.

<sup>1</sup>Y. Uesu, S. Kurimura, and Y. Yamamoto, Appl. Phys. Lett. **66**, 2165 (1995).

<sup>2</sup>V. Kirilyuk, A. Kirilyuk, and Th. Rasing, Appl. Phys. Lett. **70**, 2306 (1998).

<sup>3</sup>V. Gopalan and R. Raj, Appl. Phys. Lett. **68**, 1323 (1996).

<sup>4</sup>J. Jephagnon, Phys. Rev. B **2**, 1091 (1970).

<sup>5</sup>O. A. Aktsipetrov, A. A. Fedyanin, D. A. Klimkin, A. A. Nikulin, E. D. Mishina, A. S. Sigov, K. A. Vorotilov, M. A. C. Devillers, and Th. Rasing, Ferroelectrics **190**, 143 (1997).

<sup>6</sup>Yamada, Y.-K. Chung, M. Takahashi, and T. Ogawa, Jpn. J. Appl. Phys., Part 1 **35**, 5232 (1996).

<sup>7</sup>H. Vogt and D. Weinmann, Phys. Status Solidi A **14**, 501 (1972).

<sup>8</sup>W. L. Warren, H. N. Al-Shareef, D. Dimos, B. A. Tuttle, and G. E. Pike, Appl. Phys. Lett. **68**, 1681 (1996).

<sup>9</sup>E. D. Mishina, T. V. Misuryaev, A. A. Nikulin, Th. Rasing, and O. A. Aktsipetrov, J. Opt. Soc. Am. B **16**, 1692 (1999).

<sup>10</sup>L. D. Rotter and D. L. Kaiser, Integr. Ferroelectr. **22**, 153 (1998).